



**International Journal of Mobile Network Design and Innovation**

ISSN online: 1744-2850 - ISSN print: 1744-2869

<https://www.inderscience.com/ijmndi>

---

**Leveraging Bluetooth 5.1 location services for improved multilateration: a preliminary study on indoor asset tracking**

Miguel Roque Soares, Tiago Rocha, Duarte Oliper, Vânia Guimarães, Ricardo Santos

**DOI:** [10.1504/IJMNDI.2023.10057891](https://doi.org/10.1504/IJMNDI.2023.10057891)

**Article History:**

Received:	25 May 2023
Last revised:	26 May 2023
Accepted:	09 June 2023
Published online:	03 September 2023

---

## Leveraging Bluetooth 5.1 location services for improved multilateration: a preliminary study on indoor asset tracking

---

Miguel Roque Soares\*, Tiago Rocha, Duarte Oliper,  
Vânia Guimarães and Ricardo Santos

Fraunhofer Portugal AICOS,  
R. Alfredo Allen 455/461,  
4200-135 Porto, Portugal  
Email: miguel.roque@fraunhofer.pt  
Email: tiago.rocha@fraunhofer.pt  
Email: duarte.pereira@fraunhofer.pt  
Email: vania.guimaraes@fraunhofer.pt  
Email: ricardo.santos@fraunhofer.pt

\*Corresponding author

**Abstract:** Accurately tracking and managing indoor assets is crucial in many industries, such as healthcare, manufacturing, and warehousing. This exploratory study presents a new approach to indoor asset tracking using *Nordic Semiconductor*® innovative distance estimation techniques based on Bluetooth 5.1 physical layer updates. Our multilateration algorithm calculates the asset's exact location by leveraging distance estimates from multiple receivers over an extended period. We demonstrate the effectiveness of our system through real-world experiments conducted in an office setting, which shows that our system can locate and track assets with an average error of approximately  $\sim 2.1$  m using a BLE receptor density of approximately  $\sim 3$  per  $550\text{ m}^2$ . We also discuss our methodology, potential applications of our system, and future enhancements to improve the system's accuracy and expand its capabilities.

**Keywords:** indoor location; multilateration; BLE 5.1; radio link; RF; distance estimation.

**Reference** to this paper should be made as follows: Soares, M.R., Rocha, T., Oliper, D., Guimarães, V. and Santos, R. (2023) 'Leveraging Bluetooth 5.1 location services for improved multilateration: a preliminary study on indoor asset tracking', *Int. J. Mobile Network Design and Innovation*, Vol. 10, No. 4, pp.212–221.

**Biographical notes:** Miguel Roque Soares received his MSc in Electronics and Telecommunications Engineering from the University of Aveiro in 2020. With experience as a Hardware engineer at Barix AG, he currently works as Researcher for Embedded Hardware at Fraunhofer AICOS. His research interests include RF hardware development, EMC/EMI knowledge, Batteryless topics and Indoor Positioning Systems.

Tiago Rocha achieved a Master's degree in Computer Engineering in 2013 from Faculdade de Engenharia da Universidade do Porto. Currently working as a Researcher and Developer of Connected Things group at Fraunhofer Portugal AICOS. Previous work includes research, implementation and development in areas such as FallDetection, IndoorLocation, system architecture and supply chain management and Blockchain.

Duarte Oliper is a Researcher at the Intelligent Systems group at Fraunhofer Portugal AICOS. He is an MSc in Biomedical Engineering and his main interests are data science and machine learning. His has worked in areas such as drowsy driving prevention, indoor location, predictive maintenance, and defect detection.

Vânia Guimarães is a Researcher at the Intelligent Systems Department of Fraunhofer Portugal AICOS and a PhD student at the University of Porto. She received her MSc in Biomedical Engineering in 2011 and has been working on research ever since. Her research interests concern the areas of human motion analysis, sensor data fusion, time series analysis, and machine learning, applied to the fields of health and aging.

Ricardo Santos is a Researcher of the Intelligent Systems group at Fraunhofer Portugal AICOS. He is an MSc in Biomedical Engineering and his main interests are data science and Machine Learning for Healthcare. Currently, he is pursuing a PhD in Biomedical Engineering, focusing on improving the robustness of Machine Learning and Deep Learning to asynchronous and missing inputs.

This paper is a revised and expanded version of a paper entitled ‘Novel Bluetooth 5.1 location services for indoor asset tracking using multilateration’ presented at *Wireless Telecommunications Symposium 2023*, Boston, USA, 19–31 April, 2023.

## 1 Introduction

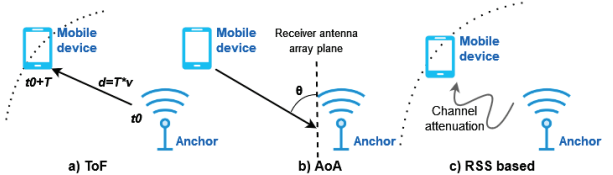
With the development of interconnected devices (Internet of Things or IoT) (De Oliveira et al., 2021), and the expansion of infrastructures such as hospitals, airports, shopping malls, libraries, and stadiums (Lam and She, 2019; Liu et al., 2007), there is an increasing demand for a continuous and interactive system to precisely localise and guide the general public. Indoor Positioning Systems (IPS) are crucial for personal and asset tracking in various industrial settings such as warehouses (Zhao et al., 2016), hospitals (Yoo et al., 2018), and industrial spaces (Flatt et al., 2015). However, indoor wireless signals are susceptible to issues such as attenuation, reflection, scattering, interference, and diffraction (De Oliveira et al., 2021; Kajioka et al., 2014), which can impact their accuracy. Despite the progress in research, standardisation for indoor location systems remains lacking (Deak et al., 2012), providing opportunities for further advancements in the field (Liu et al., 2007; Yassin et al., 2016).

There is a growing trend in using personal devices connected to WLAN/WPAN networks, leading to the creation of a large wireless sensor network (WSN) (Wang et al., 2009) that utilises technologies such as WiFi and Bluetooth low energy (BLE). Both technologies operate on the unlicensed ISM band of 2.4 GHz (Neburka et al., 2016), offering low power consumption, easy deployment, and widespread infrastructure. BLE, in particular, has been found to have advantages over WiFi for indoor positioning system (IPS) applications (Zhao et al., 2014), such as a faster scanning rate, frequency hopping, lower power consumption, and unobtrusive deployment. Various positioning techniques for Bluetooth low energy (BLE) involve estimating the distance between anchor stations with known positions and devices with variable positions (Yassin et al., 2016). The three fundamental methods are time of flight (ToF) (Liu et al., 2007), angle of arrival/departure (AoA/AoD) (Yassin et al., 2016; Liu et al., 2007), and received signal strength based (RSS-based) (see Figure 1). The latter can be further divided into two different approaches, the first being distance estimation based on channel attenuation (Zhao et al., 2014), and fingerprinting, which estimates the asset location by matching the online RSS measurement with previously mapped values (Yassin et al., 2016).

The main method for estimating distance and position in BLE-based IPS is RSS/RSSI, but there are some considerations to take into account (Lam and She, 2019). The accuracy of this method depends on the signal rate and data filters, as studied in Lam and She (2019). However, the channel response is also impacted by radio-frequency phenomena,

such as absorption, refraction, or interference, which can make it difficult to derive a deterministic formula to relate measured radio power with distance/position (Neburka et al., 2016; Faragher and Harle, 2015). To improve the position error, data filters such as median filtering (Faragher and Harle, 2015) or Kalman filtering (De Oliveira et al., 2021) can be applied. Antenna directivity is also crucial for RSS-based algorithms, as signal intensity plays a key role in their accuracy (Kajioka et al., 2014). Several studies have investigated the performance of multilateration RSS-based methods (De Oliveira et al., 2021; Dinh et al., 2021; Faragher and Harle, 2015). For example, De Oliveira et al. (2021) and Dinh et al. (2021) reported an overall system accuracy of 2.33 m and 1–2 m, respectively, with a density of 3 anchors per 70 m<sup>2</sup> and 96 m<sup>2</sup>. In contrast, Faragher and Harle (2015) achieved an accuracy of 2.5 m with a lower density of 3 anchors per 118 m<sup>2</sup>.

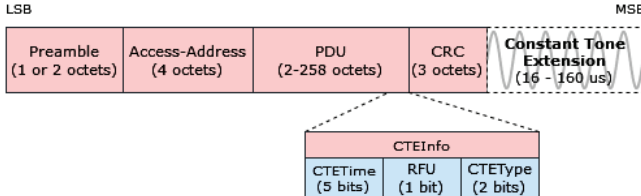
**Figure 1** Different distance/positioning methods based on Bluetooth technology (see online version for colours)



A new strategy utilising updates and optimisations from the Bluetooth 5.1 standard has been proposed to overcome some of the RSS-based constraints. Bluetooth 5.1 is an evolution of its precedent 5.0, presented by *Bluetooth SIG*© in 2019, and includes improvements to the Bluetooth core specification such as advanced Generic Attribute Profile (GATT) catching, changes on channel advertisement routine, and direction-finding capability (*Bluetooth SIG*, 2020). This latest version brings great potential to applications on IPS (Suryavanshi et al., 2019). At the link layer, a new field named Constant Tone Extension (CTE) was added to the end of the packet structure (*Bluetooth SIG*, 2020). The tone has a variable length – configured by the host controller interface (HCI) – and constant frequency, wavelength, and phase signal material. These allow for In-Phase and Quadrature (IQ) modulation to be performed (Figure 2). In addition to angle calculation, some Bluetooth radio manufacturers such as Texas Instruments© (2021) and Nordic Semiconductor© (2021) made use of this new physical update brought with BLE 5.1 to internally develop solutions to distance estimation. These new techniques make use of new properties offered by the CTE extension to compute the IQ-modulated properties based on signal propagation calculations – inverse fast-Forrier

(IFFT), phase-slope, and link-loss (RSSI) – to obtain more robust and precise distance estimations. Proprietary methods for distance estimation in BLE-based Indoor Position Systems promise easier deployment, smaller infrastructure, and more robust results in real-world scenarios compared to raw RSS-based methods that require additional data processing.

**Figure 2** New Bluetooth 5.1 packet structure embracing the CTE appendices (see online version for colours)



Therefore, the aim of this study was to assess the effectiveness and potential of the recently introduced distance estimation techniques in Bluetooth 5.1 by designing a low-cost solution for asset tracking in practical indoor settings. Signal phase processing-based methods for distance estimation is an inventive approach, as they are relatively new and have only recently been adopted as the industry standard since their introduction in 2019.

This paper explores and compares the new distance estimation methods provided by *Nordic Semiconductor*® hardware and the *nRF Connect SDK* for configuring the physical layer structure in our asset tracking solution. It also presents a proposed system architecture comprising the necessary physical components and software stack. The methods were evaluated through field tests in an active office setting to establish a baseline and benchmark. After distance estimation, a complete IT infrastructure was created including base stations, a back-end engine, and a position estimation interface. To compute asset location from the distance between the asset and base stations, we chose multilateration for its low complexity and computational cost (Jianyong et al., 2014).

The rest of the paper is organised as follows: Section 2 details the different distance methods implemented by *Nordic Semiconductor*® used in our solution; Section 3 describes the implemented system's hardware and firmware, data workflow and back-end engine; Section 4 outlines the test environment and experiments; Section 5 present the obtained results and analyses the underlying reasons for the results; lastly, Section 6 summarises the paper and suggests future work.

## 2 Distance estimation methods

For the distance estimation, functionalities available by the library *Distance Measurement* compatible with *nRF52* and *nRF53* SoC series were utilised. The library is included in the *nRF Connect SDK*. As it is pre-built for the *RTOS* operating system in C++ language, it cannot be analysed in depth (*Nordic Semiconductor*®, 2023). The Bluetooth 5.1 distance estimation feature uses IQ modulation and sampling to obtain frequency and phase attributes for the algorithm. IQ modulation converts two different magnitudes

into one signal by using a cosine function for the In-Phase signal and a sine function for the Quadrature signal, which are 90° out of phase (Naidu, 2003). The IQ signals are amplitude-modulated by manipulating I and Q magnitude vectors. Equation (3) represents the modulated signal with the corresponding In-Phase (equation (1)) and Quadrature (equation (2)) components.

$$I(t) \cdot \cos(2\pi ft) \quad (1)$$

$$Q(t) \cdot \sin(2\pi ft) \quad (2)$$

$$s(t) = I(t) \cdot \cos(2\pi ft) + Q(t) \cdot \sin(2\pi ft) \quad (3)$$

$$\begin{aligned} s(t) &= A \cdot \cos(2\pi ft + \phi(t)) = \\ &A \cdot \cos(2\pi ft) \cdot \cos(\phi(t)) - \\ &A \cdot \sin(2\pi ft) \cdot \sin(\phi(t)) \end{aligned} \quad (4)$$

The incoming signal  $s(t)$  is phase-modulated, which can be represented as in equation (4) (in an expanded form of equation (3)), where  $f$  is the carrier frequency,  $t$  is time,  $A$  the amplitude of the signal, and  $\phi(t)$  is the instantaneous phase. Based on that, Bluetooth radio when receiving the  $s(t)$  (present in the CTE appendices), performs an amplitude and phase sampling that after demodulation enables the retrieving of I and Q individual components (equation (5)).

$$\begin{aligned} I(t) &= A \cdot \cos(\phi(t)) \\ Q(t) &= -A \cdot \sin(\phi(t)) \\ A &= \sqrt{I^2 + Q^2} \quad \phi = \arctan(Q/I) \end{aligned} \quad (5)$$

### 2.1 Multi-carrier phase slope estimation (Phase)

For this method, the library measures the phase difference between the two devices at multiple carrier frequencies. The process consists of device A transmitting a signal to device B, and this one then returning the signal back to A at the same frequency. Device A measures the phase difference between the received signal and its local oscillator (*Nordic Semiconductor*®, 2023). The distance based on phase difference can be represented as in equation (6), where  $\Theta$  is the phase difference,  $f$  is the modulation frequency, and  $c$  is the speed of light (Óafsdóttir et al., 2016). It should be noted that the distance has to be smaller than the frequency wavelength.

$$\Theta = 4\pi \cdot \frac{d \cdot f}{c} \quad (6)$$

To avoid that limitation, a multicarrier phase ranging is implemented by *Nordic Semiconductor*®, where continuous wave signals are transmitted at different frequencies. Considering two frequencies ( $f_1$  and  $f_2$ ) and applying the two frequencies to equation (6), equation (7) is obtained. To improve solution resilience, more than just two frequencies are used. By crossing the results of phase differences obtained in the function of frequency, a curve graph is generated, where the slope represents the distance. This method is known as 'Phase Slope'.

$$d = \frac{c}{4\pi} \cdot \frac{\theta_2 - \theta_1}{f_2 - f_1} \quad (7)$$

## 2.2 IFFT of spectrum

Inverse fast Fourier transform (IFFT) is used to convert a signal from the frequency domain to the time domain. When converted, the distance can be obtained from the time delay constant (Wu et al., 2021). This technique is also used in reflective radar, where the delay is twice the distance between the antenna and a reflective object (round-trip delay) or just once, where two devices transmit to each other (1-way ranging mode). That is the approach implemented when two *Nordic Semiconductor*® devices running the distance estimation algorithm measure the distance between them.

## 2.3 Friis path loss (RSSI)

Friis formula relates the power level between two antennas to a function of distance and operating frequency:

$$P_r = G_t \cdot G_r \cdot \left( \frac{\lambda}{4\pi d} \right)^2 \cdot P_t \quad (8)$$

where  $G_t$  and  $G_r$  represent the gain of the transmitter and receiver antenna respectively,  $\lambda$  is the wavelength of the transmitted frequency, and  $d$  is the distance between devices. An inversely proportional relation of  $1/d^2$  between distance and received signal can be perceived. The path-loss theory shows instead that the relationship is dependent on the environment, transforming the relation into  $1/d^n$ , where  $n$  is known as the path-loss factor. This factor may vary from 1.6 to 6, with experimental measurements being used to obtain it (Zhao et al., 2014).

## 2.4 High precision (HPrecision)

As mentioned above, *Nordic Semiconductor*® keeps its library pre-compiled, so no further deterministic mathematical analysis assumptions are possible. It is based on the same IFFT of the spectrum method, with the addition of more computation in order to obtain better precision. In consequence, the processing time increases (to the order of tens of milliseconds), as well as the power consumption (*Nordic Semiconductor*®, 2023).

## 3 Architecture

The proposed indoor localisation solution allows for deployment in large buildings, requiring internal network infrastructure. Figure 3 represents the components of the system, which are described next.

### 3.1 Base station

Is the element tasked with gathering BLE signals and computing distances from the assets to be tracked (Figure 4). The base station consists of a *Nordic nRF5340\_DevKit* (DevKit) flashed with the distance measurement firmware. Connected to the DevKit, a *Raspberry Pi*, running a Python script, collects and parses the data and inserts it into the database. The antenna element plays a crucial role in the

overall system performance (Kajioka et al., 2014), factors such as directivity, gain, and sensitivity influence the coverage area and may erroneously interfere with the obtained position estimations. Based on that an external monopole antenna was deployed (instead of DevKit PCB printed antenna) to ensure an isotropic radiation pattern over the surrounding space and consequently achieve a more uniform coverage around the base station placement. A metallic plate was attached to the bottom of the antenna pole and connected to the return signal with the purpose of creating a solid “image antenna” therefore increasing the antenna gain. All the base stations were fixed to a wall at a height of approximately 2 m.

**Figure 3** System physical architecture and hierarchy (see online version for colours)

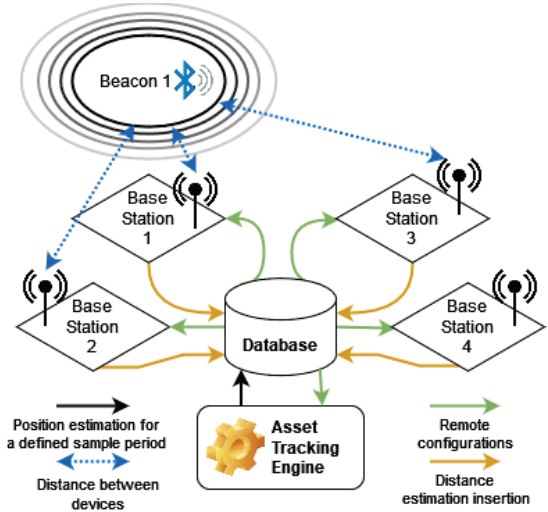
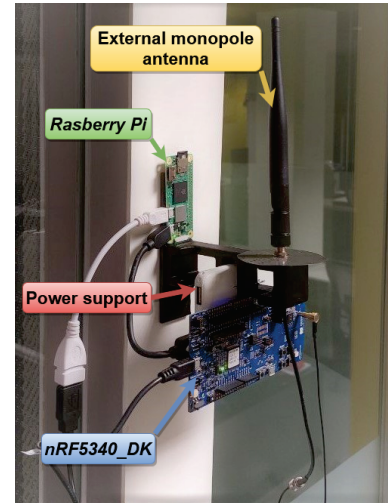


**Figure 4** Picture of base station assembly (see online version for colours)



### 3.2 Database

A server deployment capable of storing information about the asset tracking system, including information about the current state of the system and building details - dimensions, floor

data and platform-specific information about the base stations' location, media access control (MAC) address, and identifiers. The database is deployed using *MySQL* and is used by various elements of the system to query and add data about positions and distance estimation events.

### 3.3 Asset tracking engine

A Backend system on an applicational server that composes the core of the solution. The processing of localisation algorithms runs on this platform. It queries the database to fetch building and beacon information and calculates the location of assets based on data received from base stations and stores new locations in the database.

### 3.4 Beacon/Asset

Beacon and asset are different physical entities, where the beacon is the device that emits a BLE radio signal. In this context, the beacon will be linked to a specific asset (target of localisation). Therefore in the context of these experiments, they can be treated as one.

### 3.5 Information workflow

Figure 5 illustrates the main system information workflow for computing the location of assets. There are five entities represented in the flow diagram, four of them are previously explained components, and the remaining entity is the front end, used only to visualise the current state of the assets in the building. Database is the core entity that needs to be fully configured before the system's deployment. Other elements query the database for an initial configuration. Base stations need to know the addresses of all other base stations in the building and start scanning for assets and computing distances. Engine startup is similar, regarding the database queries. The base station redirects the resulting scan to the Asset Tracking engine and Database via web socket and API respectively. Engine processes the event data, if the positioning is successful, it stores the new location of the given asset in the database.

### 3.6 Software

The software ecosystem in Figure 6 has dependencies between several modules, including a base station with components, a database, and a third module that can be used for real-time asset tracking or data storage and computation during development. The real-time tracking scenario uses a server to process data and output estimated positions to the database. The development scenario uses a software infrastructure called *Playground* to run previously gathered and annotated samples and evaluate results. The core code for the system called the 'Asset tracking module', is shared between the *Playground* and the real-time tracking back-end.

### 3.7 Asset tracking module

This module performs calculations and algorithm implementation to estimate locations for each asset using input

signals, it is developed using Python and can communicate directly with the database. It can be used in real-time when deployed in the Real-time tracking back-end or in a simulation when running the playground on a local machine.

**Figure 5** System elements information workflow (see online version for colours)

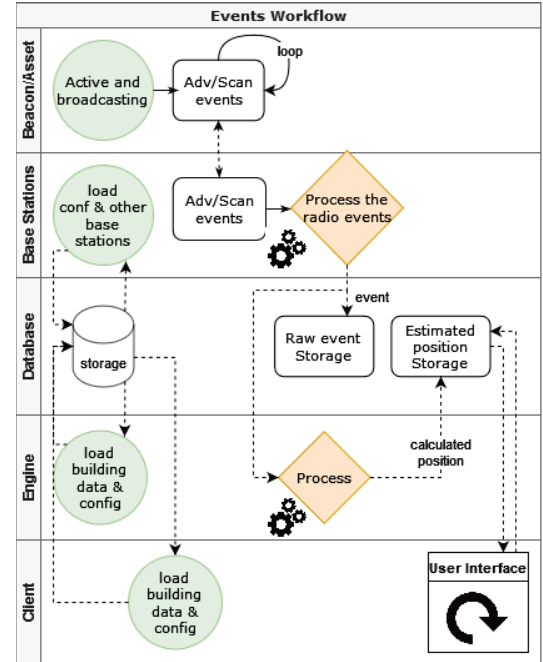
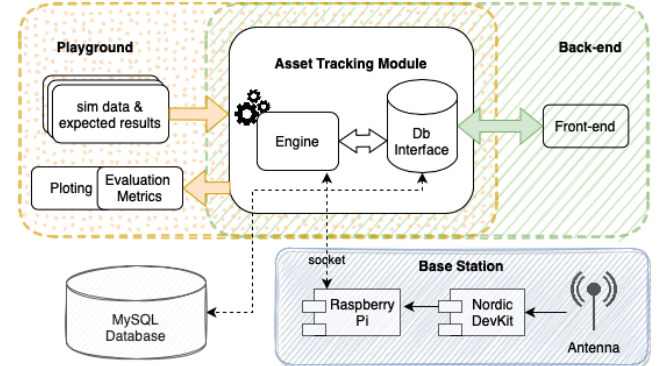


**Figure 6** Software stack (see online version for colours)



### 3.8 Playground

This project, developed using Python, is a development tool that allows running individual parts of the algorithm and location estimation mechanics in the Asset Tracking Module, with the ability to explore and evaluate results using annotations for each sample. It includes tools for signal input evaluation and interpretation, error plots, position plots on a map, sample playback with map overlay, and other useful metrics.

### 3.9 Back-end

Also a Python-based component depending on the same Asset tracking module. Using a socket, the Back-end receives

scans directly from the base station and computes a location estimation through the Asset tracking. For a proof-of-concept, a front-end is used to check the current system status and locations.

### 3.10 Database

A simple database deployment with our system infrastructure (tables/collections). Currently using MySQL due to ease of implementation and deployment.

### 3.11 Base Station(s)

A Python script is used at startup to load the database and initialise it. The communication between Raspberry and DevKit uses the serial port.

## 4 Experiments

The indoor location implementation uses a radio propagation model to calculate the distance between an asset and base stations. The first set of methodologies includes experimentation for distance estimation with a single pair of DevKits (Section 4.2), while the latter approximates the real asset tracking scenario (Section 4.3).

### 4.1 Environment

The study used an open office setting as a realistic indoor scenario, with desks, electronic devices connected by WiFi and Bluetooth, and people present to affect distance estimation accuracy. The location of the base stations and assets was recorded and compared to the ground truth. The asset's location was changed frequently during the acquisition.

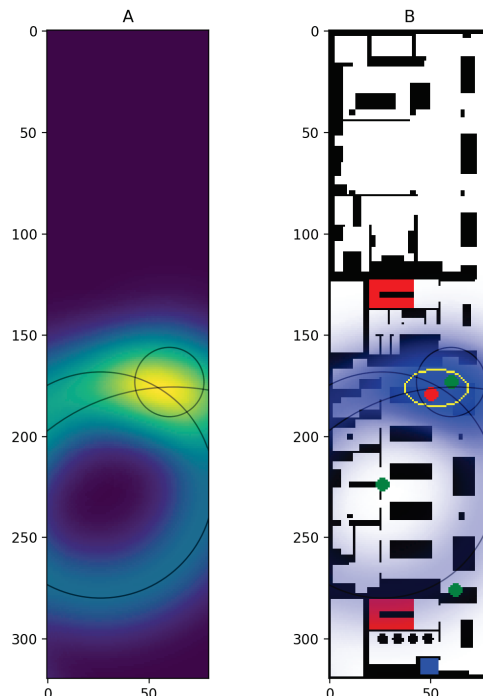
### 4.2 Distance estimation with line of sight (LoS)

In order to compare different estimation methods provided by *Nordic Semiconductor* DevKit (i.e., RSSI, Phase, IFFT, and HPrecision), distance computations were performed between a fixed base station and an asset moving away in a straight line. The asset's location was switched every 60 min (approximately), resulting in three different test distances: 5.2 m, 9.0 m, and 12.7 m. In this experiment, no obstacles were present between the asset and the fixed base station, but the circulation of people within the office was allowed. Before calculating the errors, raw distance estimations were filtered using a median filter with a sliding window of 5 samples, which removed outliers. Then, for each position, the average error was calculated. The overall average error – including all tested distances – was also calculated. To calculate the errors, the 60 s surrounding the moments when the asset position was moved were excluded. This operation allowed for the exclusion of distance estimations while the asset was moving, and to account for imprecise annotations of relocation timings.

### 4.3 Asset tracking

The aim of this experiment was to locate a single asset through time with three base stations in an indoor close-to-real-world scenario, with electromagnetic interference from other devices. Tests were performed in an open space office, having the base stations located in three corners of the space, separated by a maximum of 30 m. The placement of the base stations was planned to allow for coverage of the experimental environment, but it was not optimised any further. Figure 7(B) shows the building schematic and the location of the three base stations (green circles). The asset was placed in different positions, switched every 30–60 min, over a total of 13 h.

**Figure 7** Algorithm heatmap (A) and analysis (B). Pixelised schematic scale, where 1 pixel corresponds to 0.20 m (see online version for colours)



To locate the asset, a multilateration algorithm uses each of the aforementioned distance metrics. First, we calibrated raw distance estimations by subtracting the offsets, as recommended by *Nordic Semiconductor* (Nordic Semiconductor®, 2022a). According to *Nordic Semiconductor* (2022a), these offsets may depend on the design of the radio circuit, the antenna used, and the PCB layout, and should, therefore, be compensated. To obtain these offsets, we have calculated the average errors (i.e., the average difference between the measurement values and the actual distances) obtained in the LoS experiments (Section 4.2). Next, we applied a median filter to remove outliers, using a sliding window with 3 samples (experimentally set). Considering more than one static single measurement (as suggested on *Nordic Semiconductor* (2022a) makes the offset obtained more precise and exempted from external interference.

This was performed within a 1-min window prior to the current reading.

Then, for each base station/asset pair, the average distance of the window is computed. This distance is illustrated as the radius of the black circumferences in Figure 7. Through early experimentation, we noticed that the distance measurement errors follow a symmetric distribution around the mean – in other words, a Gaussian distribution. Therefore, for each base station connecting to the asset, Gaussian rings representing probabilities for the asset location were generated. The rings are centred on the corresponding base station, with radii equal to the average distance, a standard deviation of 15 pixels (corresponding to  $15 \times 0.20 = 3$  m), and a ring thickness of 3 m (experimentally set). The Gaussian rings corresponding to the same asset were then summed and overcast to the shape of the building schematic. The resulting matrix values were divided by the number of base stations, to normalise probability values. A threshold of 0.99 was applied to the matrix to exclude low-intensity (or low-probability) positions. Finally, the weighted average of the resulting probabilities (heatmap shown in Figure 7(A) and blue shading in Figure 7(B)) corresponds to the position estimation (centre of the white ellipse in Figure 7(B)). The standard deviations in the horizontal and vertical axis provide an expected uncertainty area for the asset location (white ellipse in Figure 7(B)).

## 5 Results and discussion

Figure 8 shows raw distance estimations and ground truth obtained in the LoS experiment described in Section 4.2. Table 1 provides a quantification of the errors, after applying median filtering to the raw data.

**Table 1** Line of sight distance estimation results

Distance method	Error 5.2 m	Error 9.0 m	Error 12.7 m	Error Total
RSSI	$-4.1 \pm 0.4$	$-6.5 \pm 0.6$	$-9.5 \pm 1.2$	$-7.7 \pm 2.1$
Phase	$10.1 \pm 0.5$	$5.9 \pm 0.6$	$13.1 \pm 0.5$	$9.7 \pm 3.4$
IFFT	$1.7 \pm 0.1$	$0.9 \pm 0.1$	$2.7 \pm 0.1$	$1.9 \pm 0.9$
HPrecision	$2.1 \pm 0.7$	$2.0 \pm 0.1$	$3.0 \pm 0.1$	$2.5 \pm 0.5$

Errors shown in m as average  $\pm$  standard deviation.

Analysis reveals that the methods of Phase and RSSI provide the worst distance estimation results, with 9.7 m and  $-7.7$  m total average error, respectively. All the errors in this scenario were positive, with the exception of the RSSI method. In the case of RSSI, the mean absolute error increased from 4.1 m to 9.5 m when increasing the distance from 5.2 m to 12.7 m. This is in accordance with the expected path-loss behaviour for RSS-based methods (Section 2.3) because the path-loss factor considered by the algorithm is static and possibly not adequate for the environment of this work. The dispersion of the RSSI method's errors was very high (as can be visualised in Figure 8), but the median filter attenuated this limitation, resulting in an error dispersion lower than the Phase method. The Phase method revealed the highest offset and error dispersion overall, with errors varying dramatically with distance (from 5.9 m to 13.1 m). This error is expected

since the measurement is based on phase propagation delay – any reflection will always have a greater phase difference when compared to the LoS path (Óafsdóttir et al., 2016). The errors of the IFFT and HPrecision remained under 3 m for all tested conditions, with standard deviations of less than 1 m denoting higher consistency of both methods. Although we reported the results of a single base station/asset pair in this LoS experiment, the other base stations were already mounted in the office. The orchestration of the connections between each pair asset/base station resulted in momentary connection loss with the reported base station, which justifies the lack of information in some of the periods shown in Figure 8. The distance estimation process is divided into two phases: an initial synchronisation where the Nordic devices exchange packets between them, and a second part of distance measurement. This process can be configured through variable settings like advertising and scan window period, time-slot between measurements, or even events' queue limit count (Nordic Semiconductor®, 2022a). The phenomenon detected shows that some synchronisation settings must be optimised in order to avoid these blindness periods in the future. To evaluate the results of the asset tracking solution described in Section 4.3, we set up an experiment that intended to simulate a real-world scenario. Table 2 represents an overview of the location results for each of the provided distance metrics after applying the correction for the offsets mentioned in Section 4.3.

**Table 2** Asset tracking results

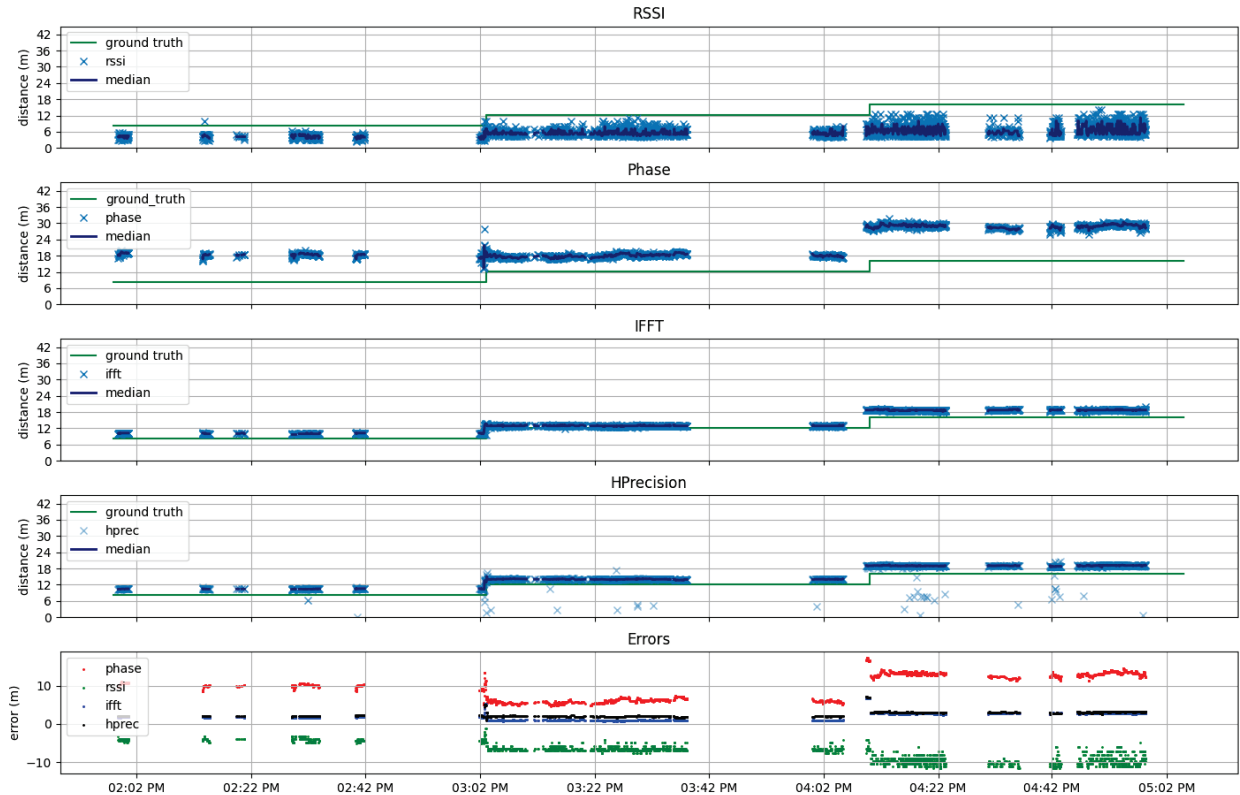
Method	RSSI	Phase	IFFT	HPrecision
Avg	$6.4 \pm 5.0$	$3.6 \pm 2.5$	$2.5 \pm 2.1$	$2.1 \pm 1.6$
Error(m)				
Avg	$6.3 \pm 5.1$	$3.5 \pm 2.4$	$2.4 \pm 2.0$	$2.1 \pm 1.5$
Error*(m)				
Location area( m <sup>2</sup> )	$35.4 \pm 14.9$	$22.8 \pm 16.1$	$22.3 \pm 8.0$	$20.0 \pm 7.3$
Location OK %	42.1	30.6	69.0	80.7
Dataset time(h)		13		
#Events			36683	

Errors shown as average  $\pm$  standard deviation. \*Excluding 60 s before and after asset position change.

In this table, average error metrics represent the distance between the centre of the estimated ellipse and the actual ground truth position (with and without excluding a window of 60 s before and after asset position changes). The average error with a 1 min exclusion window thus denotes the errors measured while the asset was static.

The 'Location Area' metric presented in Table 2 represents the average of the area of the ellipse for all processed positions, being thus a measurement of location certainty. 'Location OK' is a percentage of the processed positions where the ground truth lies inside the ellipse. This provides a rough indication of proximity to the ground truth, since the estimated position may be relatively close to the ground truth without being inside the ellipse. The dataset used for this preliminary evaluation had a total duration of 13 h, 14 different asset locations, and 36683 events reported. The best-performing result was achieved using the HPrecision method, with an average error of  $2.1 \pm 1.6$  m, followed by the IFFT method with a slightly higher

**Figure 8** Line of sight distance estimation experiment. Ground truth distances (green), distance estimations provided by each of the methods (light blue), and estimated distances after filtering (dark blue) are shown. The last graph shows the differences between estimated and ground truth distances (see online version for colours)



error of  $2.5 \pm 2.1$  m. This is the most comparable metric with other studies. The proposed ellipse area provides useful insight into the solution's performance within this controlled scenario, but it is not a sufficiently reliable metric for comparison with other studies or scenarios. The average size of the ellipse was also smaller for the HPrecision input, with a  $20.0 \text{ m}^2$  average area. These results showed that not only the centre of the ellipse was on average closer to the real position, but the area of the estimation was also more compact. Moreover, the estimated ellipse contained the ground truth more often in the HPrecision distance, totaling 80.7% of the time. The RSSI measurements, contrarily, revealed the least consistent and accurate location measurements as denoted by the highest location errors overall. The performances reported in our study were consistent with *Nordic* documentation concerning the expected performance of the different distance estimation methods (*Nordic Semiconductor*®, 2022b). Although in this study no specific efforts were taken to optimise location estimates (i.e., we used a standard multilateration approach), these results show localisation of assets with errors that are already compatible with real-world requirements to support asset management with room-level accuracy. The current implementation approach does not ensure real-time estimations of the asset position, but this should not be a critical issue for the intended real-world application, as the assets usually stay in the same position for hours at a time. This issue may still be considered and improved in the future.

Besides environmental factors, other possible causes for error currently include:

- asset tracking module factors, nominally low-complexity algorithms may under-analyse important data aspects
- the small dataset hinders the optimisation of the algorithm at this stage and may lead to bias
- although our LoS estimations can be considered more realistic and challenging, the offsets considered as an input for the localisation algorithm should be determined using a reference distance of 60 cm between the devices according to *Nordic* (*Nordic Semiconductor*®, 2021)
- non-optimal base station placement. The current placement has two base stations sharing the vertical axis of the schematic, which may have led to higher errors on the horizontal axis. Besides that, the base stations were placed in corners, which may change the radiation pattern
- annotation errors, namely imprecise annotation of timings, can negatively impact the results
- schematic resolution scale uncertainty of 0.20 m
- schematic not yet being used as input in the location processing
- most-likelihood area for asset position can be improved – from an ellipse to a more accurate post-thresholding cloud

- *nRF Distance Measurement* library settings for synchronisation and events queue control between *Nordic* devices require more experimentation for better system behaviour in order to avoid significant time slots without events.

These and other aspects should be taken into account to improve localisation performance. For instance, combining the results provided by the different metrics could be a promising way forward. Moreover, the impact of obstacles could be reduced by taking into account the building schematics information. Applying more dynamic filtering approaches, such as Kalman filters, could also improve the results. Base station placement is critical and could be improved with further knowledge of the building and construction materials.

## 6 Conclusion

In this initial study, we assessed the capabilities of novel Bluetooth 5.1 distance estimation techniques for indoor localisation. The HPrecision metric yielded the best outcomes, achieving an average positioning error of  $2.1 \pm 1.6$  m after using a standard multilateration algorithm. The results were obtained in a challenging indoor setting with obstacles (e.g., people and objects) and possible interference from other IoT devices. Although we did not incorporate any specific optimisations to exploit the collected data, the obtained results are already compatible with numerous real-world applications, demonstrating an intriguing correlation between accuracy and required infrastructure size. The findings provide a promising foundation for future optimisation. Regarding future work, we plan to incorporate more data volume and diversity to

- completely comprehend the factors that can influence accuracy
- optimise the localisation hyperparameters (e.g., via a grid search)
- locate multiple assets concurrently using more than three base stations
- execute localisation for multiple floors
- optimise base station placement.

A market-ready solution can benefit from integrating with outdoor localisation (e.g., Google Maps) and having more infrastructure deployment scalability by decreasing hardware components and computing expenses.

## Acknowledgement

This paper is a result of the project ConnectedHealth (n.º 46858), supported by Competitiveness and Internationalisation Operational Programme (POCI) and Lisbon Regional Operational Programme (LISBOA 2020), under the PORTUGAL 2020 Partnership Agreement, through the European Regional Development Fund (ERDF).

## References

- Bluetooth SIG (2020) Core Specification 5.1, <https://www.bluetooth.org/docman/handlers/> (Accessed 8 November, 2022).
- De Oliveira, L.S., Rayel, O.K. and Leitao, P. (2021) ‘Low-cost indoor localization system combining multilateration and Kalman filter’, 2021 IEEE 30th International Symposium on Industrial Electronics (ISIE), June, IEEE, pp.1–6
- Deak, G., Curran, K. and Condell, J. (2012) ‘A survey of active and passive indoor localisation systems’, *Computer Communications*, Vol. 35, No. 16, pp.1939–1954.
- Dinh, T.M.T., Duong, N.S. and Nguyen, Q.T. (2021) ‘Developing a novel real-time indoor positioning system based on BLE beacons and smartphone sensors’, *IEEE Sensors Journal*, Vol. 21, No. 20, pp.23055–23068.
- Faragher, R. and Harle, R. (2015) ‘Location fingerprinting with bluetooth low energy beacons’, *IEEE Journal on Selected Areas in Communications*, Vol. 33, No. 11, pp.2418–2428.
- Flatt, H., Koch, N., Rücker, C., Gönter, A. and Jasperneite, J. (2015) ‘A context-aware assistance system for maintenance applications in smart factories based on augmented reality and indoor localization’, 2015 IEEE 20th Conference on Emerging Technologies and Factory Automation (ETFA), September, IEEE, pp.1–4.
- Jianyong, Z., Haiyong, L., Zili, C. and Zhaojun, L. (2014) ‘RSSI based Bluetooth low energy indoor positioning’, 2014 International Conference on Indoor Positioning and Indoor Navigation (IPIN), 27–30 October, 2014, IEEE, Busan, pp.526–533.
- Kajioka, S., Mori, T., Uchiya, T., Takumi, I. and Matsuo, H. (2014, October). Experiment of indoor position presumption based on RSSI of Bluetooth LE beacon’, 2014 IEEE 3rd Global Conference on Consumer Electronics (GCCE), 7–10 October, 2014, IEEE, Tokyo, Japan, pp.337–339.
- Lam, C. H. and She, J. (2019) ‘Distance estimation on moving object using BLE beacon’, 2019 International Conference on Wireless and Mobile Computing, Networking and Communications (WiMob), October, IEEE, pp.1–6.
- Liu, H., Darabi, H., Banerjee, P. and Liu, J. (2007) ‘Survey of wireless indoor positioning techniques and systems’, *IEEE Transactions on Systems, Man, and Cybernetics, Part C (Applications and Reviews)*, Vol. 37, No. 6, pp.1067–1080.
- Naidu, P.S. (2003) *Modern Digital Signal Processing: An Introduction*, Alpha Science Int'l Ltd., ISBN: 978-1842651339.
- Neburka, J., Tlamsa, Z., Benes, V., Polak, L., Kaller, O., Bolecek, L. and Kratochvil, T. (2016) ‘Study of the performance of RSSI based Bluetooth Smart indoor positioning’, 2016 26th International Conference Radioelektronika (RADIOELEKTRONIKA), 19–20 April, 2016, IEEE, Kosice, Slovakia, pp.121–125.
- Nordic Semiconductor©(2021) nRF Asset Tracker, [https://developer.nordicsemi.com/nRF\\_Connect\\_SDK/doc/latest/nrf/libraries/](https://developer.nordicsemi.com/nRF_Connect_SDK/doc/latest/nrf/libraries/) (Accessed 10 October, 2022).
- Nordic Semiconductor©(2023) Nordic Distance Measurement library, [https://developer.nordicsemi.com/nRF\\_Connect\\_SDK/doc/latest/nrfxlib/nrf\\_dm/](https://developer.nordicsemi.com/nRF_Connect_SDK/doc/latest/nrfxlib/nrf_dm/) (Accessed 4 January, 2023).
- Nordic Semiconductor©(2022a) Bluetooth: nRF Distance Measurement with Bluetooth LE discovery, [https://developer.nordicsemi.com/nRF\\_Connect\\_SDK/doc/latest/nrf/](https://developer.nordicsemi.com/nRF_Connect_SDK/doc/latest/nrf/) (Accessed 1 December, 2022).

- Nordic Semiconductor©(2022b) Introduction to Nordic Distance Toolbox, [https://devzone.nordicsemi.com/cfs-file/\\_key/support-attachments/](https://devzone.nordicsemi.com/cfs-file/_key/support-attachments/) (Accessed January 10, 2023).
- Óafsdóttir, H., Ranganathan, A. and Capkun, S. (2017) ‘On the security of carrier phase-based ranging’, *Proceedings of the 19th International Conference on Cryptographic Hardware and Embedded Systems-CHES 2017*, 25–28 September, Taipei, Taiwan, Springer International Publishing, pp.490–509.
- Suryavanshi, N.B., Viswawardhan Reddy, K. and Chandrika, V.R. (2019) ‘Direction finding capability in Bluetooth 5.1 standard’, *Ubiquitous Communications and Network Computing: Second EAI International Conference*, 8–10 February, Bangalore, India, Proceedings 2, Springer International Publishing, pp.53–65.
- Texas Instruments©(2021) RF-RANGE-ESTIMATOR TI RF Range Estimator, <https://www.ti.com/tool/RF-RANGE-ESTIMATOR> (Accessed 16 October, 2022).
- Wang, X., Bischoff, O., Laur, R. and Paul, S. (2009). Localization in wireless ad-hoc sensor networks using multilateration with RSSI for logistic applications’, *Procedia Chemistry*, Vol. 1, No. 1, pp.461–464.
- Wu, Y., Joram, N. and Hach, R.T. (2021) ‘Quantitative comparison of distance estimation performance between TLS-MP and IFFT methods in IEEE 802.15. 4a channel models using PSFM radar technique’, *2021 International Conference on Indoor Positioning and Indoor Navigation (IPIN)*, 29 November – 2 December, IEEE, Llorente de Mar, Spain, pp.1–7.
- Yassin, A., Nasser, Y., Awad, M., Al-Dubai, A., Liu, R., Yuen, C. and Aboutanios, E. (2016) ‘Recent advances in indoor localization: a survey on theoretical approaches and applications’, *IEEE Communications Surveys and Tutorials*, Vol. 19, No. 2, pp.1327–1346.
- Yoo, S., Kim, S., Kim, E., Jung, E., Lee, K.H. and Hwang, H. (2018) ‘Real-time location system-based asset tracking in the healthcare field: lessons learned from a feasibility study’, *BMC medical Informatics and Decision Making*, Vol. 18, pp.1–10.
- Zhao, X., Xiao, Z., Markham, A., Trigoni, N. and Ren, Y. (2014) ‘Does BTLE measure up against WiFi? A comparison of indoor location performance’, *European Wireless 2014; 20th European Wireless Conference*, 14–16 May, 2014, VDE, Barcelona, Spain, pp.1–6.
- Zhao, Z., Fang, J., Huang, G.Q. and Zhang, M. (2016) ‘iBeacon enabled indoor positioning for warehouse management’, *2016 4th International Symposium on Computational and Business Intelligence (ISCBI)*, 5–7 September, 2016, IEEE, Olten, Switzerland, pp.21–26.